

Numerical investigations on interactions between tangles of quantized vortices and second sound

Citation for published version (APA):

Penz, H. R., Aarts, R. G. K. M., & Waele, de, A. T. A. M. (1995). Numerical investigations on interactions between tangles of quantized vortices and second sound. *Physical Review B: Condensed Matter*, 51(17), 11973-11976. <https://doi.org/10.1103/PhysRevB.51.11973>

DOI:

[10.1103/PhysRevB.51.11973](https://doi.org/10.1103/PhysRevB.51.11973)

Document status and date:

Published: 01/01/1995

Document Version:

Publisher's PDF, also known as Version of Record (includes final page, issue and volume numbers)

Please check the document version of this publication:

- A submitted manuscript is the version of the article upon submission and before peer-review. There can be important differences between the submitted version and the official published version of record. People interested in the research are advised to contact the author for the final version of the publication, or visit the DOI to the publisher's website.
- The final author version and the galley proof are versions of the publication after peer review.
- The final published version features the final layout of the paper including the volume, issue and page numbers.

[Link to publication](#)

General rights

Copyright and moral rights for the publications made accessible in the public portal are retained by the authors and/or other copyright owners and it is a condition of accessing publications that users recognise and abide by the legal requirements associated with these rights.

- Users may download and print one copy of any publication from the public portal for the purpose of private study or research.
- You may not further distribute the material or use it for any profit-making activity or commercial gain
- You may freely distribute the URL identifying the publication in the public portal.

If the publication is distributed under the terms of Article 25fa of the Dutch Copyright Act, indicated by the "Taverne" license above, please follow below link for the End User Agreement:

www.tue.nl/taverne

Take down policy

If you believe that this document breaches copyright please contact us at:

openaccess@tue.nl

providing details and we will investigate your claim.

Numerical investigations on interactions between tangles of quantized vortices and second sound

Heli Penz, Ronald Aarts, and Fons de Waele

Physics Department, Eindhoven University of Technology, P.O. Box 513, NL-5600 MB Eindhoven, The Netherlands

(Received 16 November 1994)

The reconnecting vortex-tangle model is used to investigate the interaction of tangles of quantized vortices with second sound. This interaction can be expressed in terms of an effective line-length density, which depends on the direction of the second-sound wave. By comparing the effective line-length densities in various directions the tangle structure can be examined. Simulations were done for flow channels with square and circular cross sections as well as for slits. The results show that in all these cases the tangles are inhomogeneous in direction as well as in space. The calculated inhomogeneities are in agreement with experiment.

I. INTRODUCTION

During the last forty years the phenomenon of vortices in superfluid helium has been a topic of considerable interest.¹ Generally the measurements in this field can be divided into three types: determination of gradients of intrinsic properties (such as temperature, pressure, or chemical potential), ion-mobility measurements, and second-sound measurements. This paper deals with the interaction of second sound with vortices, as in vortex tangles. By measuring in different directions differences in the structure of the tangle can be seen. Such an experiment has been performed by Wang, Swanson, and Donnelly² in a tube with a square cross section.

Numerical simulations are very useful in the study of vortices. By solving the equations of motion of the vortices it is possible to calculate the development of a tangle in time. This has been done by Schwarz,³ and in our group by Aarts and de Waele.⁴ The results of these calculations are in good agreement with experimentally observed flow properties. As a follow-up of the work by Aarts and de Waele second-sound interactions have been implemented in the simulation program in order to calculate the structures of tangles in different flow systems.

Since in simulations the detailed structure of the tangle is completely known this method can be used to examine the structure of the vortex tangles more thoroughly. With the results it is possible to reexamine some of the earlier experiments in which the vortex tangles were treated as homogeneous.^{5,6}

II. THEORY

A. Vortices

The equation of motion of single vortices is well known.¹ This makes it possible to perform numerical simulations of the development of complicated vortex structures. Since the complete equations require a considerable amount of computing time Schwarz³ has introduced the reconnecting vortex tangle model. This model contains two basic elements. The first element is a simplified equation for the core velocity \vec{v}_L

$$\vec{v}_L = \vec{v}_{sl} + \alpha \vec{s}' \times (\vec{v}_n - \vec{v}_{sl}), \quad (1)$$

in which α is the friction coefficient, \vec{s}' the unit vector, tangent to the vortex, \vec{v}_n the velocity of the normal component, and \vec{v}_{sl} the self-induced velocity of the vortex, given by

$$\vec{v}_{sl} = \vec{v}_{se} + \beta \vec{s}' \times \vec{s}'', \quad (2)$$

with \vec{s}'' the second derivative of the vortex line $\vec{s}(\xi)$, which is parametrized with the arc length ξ , and β a term that depends on the local radius of curvature R

$$\beta = c \frac{\kappa}{4\pi} \ln \frac{R}{a_0}. \quad (3)$$

Here c is a correction term of order one, $\kappa = 9.898 \times 10^{-8}$ m²/s the quantum of circulation, and $a_0 = 0.1$ nm the core diameter. The second element of the model is the reconnection principle which takes into account the interaction between different vortex lines. If two vortex-line elements approach within a certain distance they break open and reconnect. In our group this model has been implemented by Aarts.⁷

B. Second sound and vortices

Second-sound waves are attenuated by vortices.⁸ This attenuation can be derived from the wave equation for second sound. If all other dissipative processes are neglected, and assuming that the wave causes only small deviations from equilibrium, this wave equation is

$$\frac{\partial^2 \vec{v}'}{\partial t^2} - u_2^2 \nabla^2 \vec{v}' + \frac{\rho}{\rho_n \rho_s} \frac{\partial \vec{F}_{sn}}{\partial t} = 0. \quad (4)$$

In this equation t is time, ρ is the total fluid density, and ρ_n and ρ_s are the normal and superfluid densities respectively, \vec{v}' is the variation in the velocity difference between the normal and the superfluid component, while u_2^2 is the square of the second-sound velocity given by

$$u_2^2 = \frac{\rho_s s^2 T}{\rho_n c_V}. \quad (5)$$

Here s is the entropy and c_V the specific heat in a constant volume, both per unit mass. The time-averaged force density \vec{F}_{sn} is the total drag force per unit volume on the superfluid

$$\vec{F}_{sn} = \frac{1}{V} \overline{\int_{\mathcal{C}} \vec{f}_D d\xi} \quad (6)$$

or

$$\vec{F}_{sn} = -\frac{\alpha\rho_s\kappa}{V} \overline{\int_{\mathcal{C}} \vec{s}' \times [\vec{s}' \times (\vec{v}_n - \vec{v}_{sl})] d\xi}, \quad (7)$$

where the integration is over the vortex lines in a volume V . The horizontal lines indicate time averaging. Close to the critical velocity the average line distance is on the order of the dimensions of the flow channel.⁴ There is no region in the tube which contains many vortex lines but is small compared to the scale of the flow or of the container. Only the time average of \vec{F}_{sn} has a local character. In Eq. (6) and (7) \vec{F}_{sn} depends on the particular choice of the volume V . In this paper two types of volumes V are considered: one which covers the entire volume of the flow channel, and one which contains only the inner region of the channel, excluding the regions near the walls. This will be discussed later.

The wave equation can be solved if \vec{F}_{sn} is expressed in terms of \vec{v}' . Assuming that the frequency of the second-sound wave is large enough the disturbance in the tangle due to the wave is small. In that case the mutual friction force can also be seen as consisting of an equilibrium value \vec{F}_0 with a small variation \vec{F}' due to the wave

$$\vec{F}_{sn} = \vec{F}_0 + \vec{F}'. \quad (8)$$

The wave equation (4) represents actually three equations in three directions. The dissipation is determined by the force in the direction of the velocity, so only the equation for that direction must be considered. The variation in the mutual friction force density due to second sound, F'_i , in that particular direction is

$$F'_i = \alpha\rho_s\kappa v' L_i, \quad (9)$$

with the effective line-length density L_i defined by

$$L_i = \frac{1}{V} \int_{\mathcal{C}} \sin^2 \theta d\xi, \quad (10)$$

in which the index i represents the direction of the second-sound wave. The angle θ is the angle between a line element $d\xi$ of the vortex and this direction of propagation. For second-sound waves parallel and perpendicular to the applied flow L_i is directly related to the anisotropy measures I_{\parallel} and I_{\perp} which were introduced by Schwarz.³ If a second-sound wave is transmitted perpendicular to a vortex line L_i equals the vortex line-length density L . Usually this is not the case, therefore L_i will be called the effective line-length density. The relationship between L_i and L is determined by the $\sin^2 \theta$ term in Eq. (10). From this it follows that

$$L = \frac{1}{2}(L_x + L_y + L_z), \quad (11)$$

with x , y , and z representing three mutually perpendicular directions. The effective line-length density L_i can easily be calculated in numerical simulations, since in that case all angles θ can be calculated from the direction of the second-sound wave and the orientation of the line elements $d\xi$. Substituting Eq. (9) in (4) gives

$$\frac{\partial^2 v'}{\partial t^2} - u_2^2 \vec{\nabla}^2 v' + \frac{\alpha\rho_s\kappa}{\rho_n} L_i \frac{\partial v'}{\partial t} = 0. \quad (12)$$

TABLE I. Simulation parameters, l is the periodicity length, d the diameter of the circular tube, and w is the width of the slit. In the case of the slit periodicity was used parallel and perpendicular to the flow.

Geometry	v_{ns} (m/s)	Inner volume
Square	0.314	$50 \times 50 \times 50 \mu\text{m}^3$
Circular	0.314	$d = 50 \mu\text{m}$ $l = 50 \mu\text{m}$
Slit	0.079	$w = 50 \mu\text{m}$ $l = 50 \mu\text{m}$

This equation can be solved by substituting a wave with frequency ω and complex wave number $k = k_0 + i\alpha_i$ for v'

$$v' = v'_0 \exp(ikx - i\omega t). \quad (13)$$

From this substitution follows a dispersion relation. Solving the imaginary part of this relation gives the attenuation of second sound α_i in the presence of vortices

$$\alpha_i = \frac{\alpha\rho_s\kappa}{2u_2\rho_n} L_i. \quad (14)$$

The overall damping of the second-sound wave is also determined by the variation of the second-sound amplitude in the channel. The case treated here applies to a homogeneous wave. In resonant systems the lowest-order mode mainly senses the center of the cell which would correspond to the vortex density in the center of the channel. The high-order modes detect the vortices in the entire channel. The homogeneous sound wave describes also the important case of planar second-sound waves, e.g., in flow channels with a diameter which is much larger than the viscous penetration depth.¹¹ The viscous penetration depth typically is $5 \mu\text{m}$ at 100 Hz.

III. SIMULATIONS

Equation (10) has been used to calculate L_i in vortex tangles in the three main directions. In all cases the applied flow was parallel to the z axis, along which periodic boundary conditions were applied. Simulations have been done for square tubes, circular tubes, and slits. For circular tubes and slits these simulations were carried out for both a flat and a Poiseuille normal-component flow profile. The simulation parameters are given in Table I.

To examine the influence of the presence of the walls on the tangle structure the (effective) line-length densities were determined over the total simulation volume as well as over a smaller volume in the center of the tube. This "inner volume" had the same shape as the total simulated geometry. In Fig. 1 the simulated geometries and their respective inner volumes are shown.

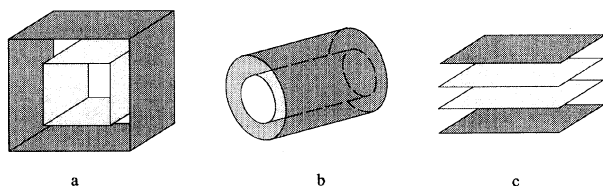


FIG. 1. The simulated geometries with their inner volumes, (a) the square tube (b) the circular tube, and (c) the slit.

TABLE II. Apparent and total line-length densities in different geometries, t and i stand, respectively, for the averages over the total and inner volume. The subscripts x , y , and z stand for the apparent line-length densities in, respectively, the x , y , and z direction.

Geometry	profile		L ($10^{-2} \mu\text{m}^{-2}$)	L_x ($10^{-2} \mu\text{m}^{-2}$)	L_y ($10^{-2} \mu\text{m}^{-2}$)	L_z ($10^{-2} \mu\text{m}^{-2}$)
Square	Flat	t	1.76 ± 0.15	1.04 ± 0.10	1.02 ± 0.09	1.44 ± 0.13
		i	2.05 ± 0.29	1.23 ± 0.18	1.16 ± 0.19	1.71 ± 0.29
Circular	Flat	t	1.7 ± 0.2	1.0 ± 0.1	1.0 ± 0.1	1.4 ± 0.1
		i	2.0 ± 0.3	1.2 ± 0.2	1.2 ± 0.2	1.7 ± 0.3
Circular	Pois.	t	0.54 ± 0.16	0.33 ± 0.10	0.33 ± 0.10	0.41 ± 0.14
		i	0.24 ± 0.16	0.14 ± 0.09	0.14 ± 0.09	0.21 ± 0.14
Slit	Flat	t	1.10 ± 0.13	0.62 ± 0.09	0.72 ± 0.09	0.86 ± 0.10
		i	1.17 ± 0.17	0.72 ± 0.13	0.72 ± 0.11	0.90 ± 0.14
Slit	Pois.	t	0.47 ± 0.12	0.28 ± 0.08	0.28 ± 0.07	0.38 ± 0.10
		i	0.34 ± 0.10	0.28 ± 0.09	0.24 ± 0.07	0.15 ± 0.06

IV. RESULTS

The simulations are used to determine the effective and total line-length densities in the systems presented in Fig. 1. The averages are given in Table II.

Since $L_z > L_x, L_y$ in all cases the vortices prefer to orient perpendicular to the applied flow in all geometries. This effect is most clearly illustrated by Schwarz⁹ in the case of a vortex ring. The fact that the vortices show only a preference for the perpendicular direction and do not align totally is caused by the reconnection process, which tends to randomize the tangle.

The results for the square tube can be compared with the experiments of Wang, Swanson, and Donnelly.² They determined that the ratio $L_{x,y}/L_z$ for the square tube is equal to 0.7. This is in agreement with our results which give $L_{x,y}/L_z = 0.7 \pm 0.1$.

From the simulations for the square and circular tubes it follows, as to be expected, that the tangle is homogeneous in the direction perpendicular to the flow, independent of the boundaries. This means that in these ge-

ometries the total line-length density can be determined by measuring the effective line-length density in only two directions, one parallel and one perpendicular to the applied flow.

In the case of circular tubes an interesting difference is found between the flat flow profile and Poiseuille flow. In the latter case the total line-length density is much smaller than with a flat flow profile. Furthermore for the flat flow profile the vortices are homogeneously distributed over the tube, while for the Poiseuille flow they tend to concentrate in a region close to the boundaries, as is illustrated in Fig. 2. This effect is explained by the work of Samuels.¹⁰ He showed that the vortices tend to accumulate in a region where the applied normal flow velocity is equal to the applied superfluid velocity. In our case this region lies at the boundaries.

For the slit with flat normal velocity flow profile the tangle is homogeneous in the two directions perpendicular to the flow in the inner volume, while this is not the case for the total volume. This is caused by the fact that the vortex lines are connected perpendicular to the

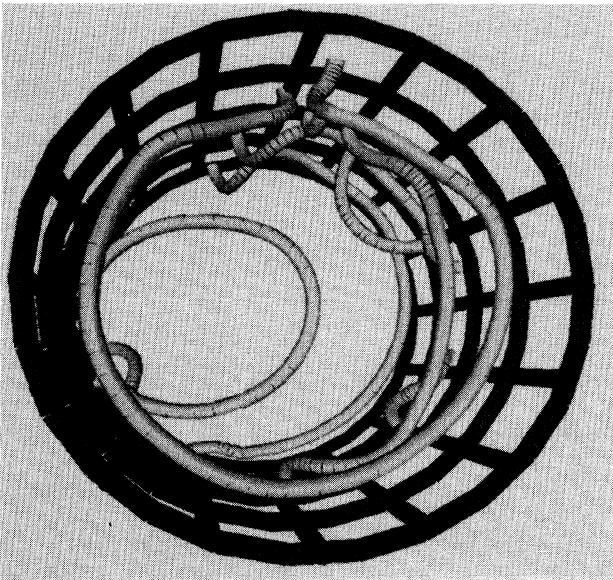


FIG. 2. Example of the vortex configuration in a circular tube with Poiseuille flow in equilibrium. The solid wall of the tube is here represented by a grid.

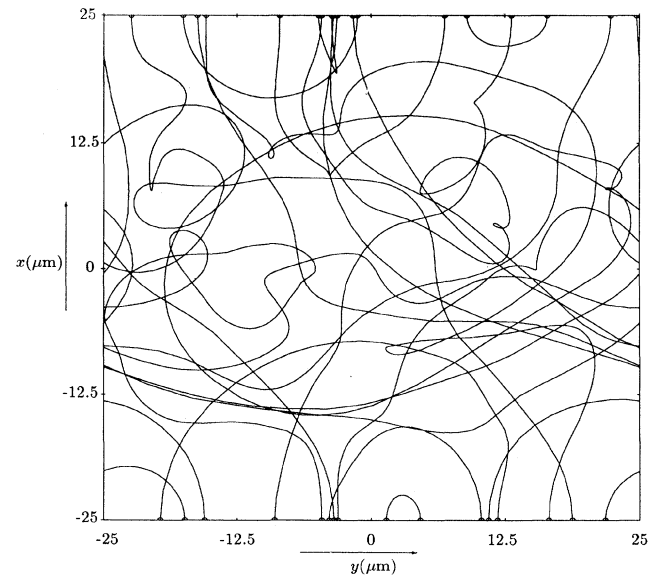


FIG. 3. x - y projection of the vortex tangle in a slit with flat flow profile. The boundaries of the slit lay at $x = \pm 25 \mu\text{m}$, while the boundaries of the inner volume lay at $x = \pm 12.5 \mu\text{m}$.

plates. Figure 3 shows an x - y projection of this situation, in which this effect is illustrated.

The opposite result is found for the slit with Poiseuille flow. Here in the inner volume the tangle is inhomogeneous perpendicular to the flow, while over the total volume it seems to be homogeneous. This means that the preferred orientation in the center is opposite to the one near the boundaries. Figure 4 represents a typical example of the tangle in the steady state. It shows that the vortices tend to balloon to the boundaries. In the center of the channel they are aligning perpendicular to the plates, while at about $10 \mu\text{m}$ from the boundaries there is a region where they are oriented preferably parallel to the plates. At the boundaries the orientation is perpendicular to the plates as usual.

The differences between the results for the inner and total volume for both the flat and parabolic flow profile in the slit make it difficult to predict whether two second-sound measurements will be sufficient to determine the total line-length density in the system. It is therefore necessary to examine this phenomenon further in experiments.

With the effective line length the second-sound attenuation can be determined using Eq. (14). In this equation the term $(\alpha\rho\kappa)/(2u_2\rho_n)$ depends only on temperature. For a temperature of 1.7 K the value is 0.14×10^{-8} m. For L_i -values of 0.001 – $0.017 \mu\text{m}^{-2}$ this implies inverse attenuation lengths ranging from 50 cm^{-1} to 4 cm^{-1} .

V. CONCLUSIONS

Numerical simulations can be used to examine the properties of second-sound interaction with vortex tangles in detail. The results show inhomogeneities in vortex tangles both in density and orientation. The vortices prefer to orient in the plane perpendicular to the applied flow, in agreement with the results of Wang, Swanson, and Donnelly.²

As expected there is no difference between the two directions perpendicular to the flow in square and circular tubes. This means that the total line-length density in these channels can be determined by measurements in only two directions. For slits measurements should be done in all three directions to determine the total line-length density correctly.

Early second-sound experiments^{5,6} have been per-

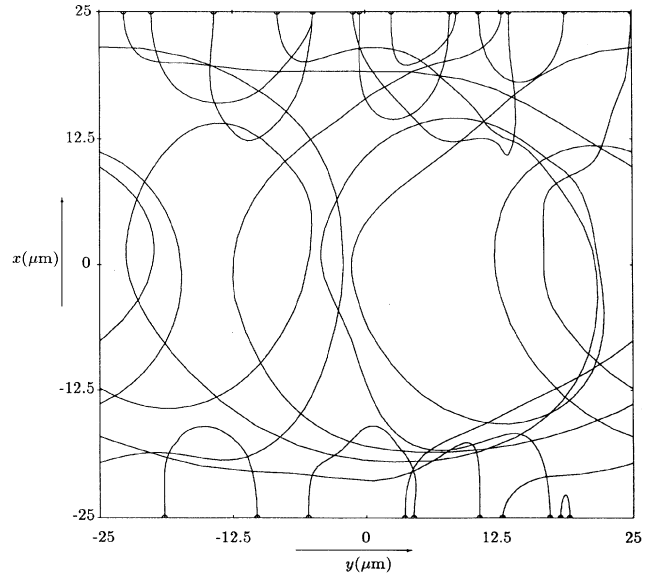


FIG. 4. The same projection as in Fig. 3 but now for a slit with Poiseuille profile.

formed measuring in only one direction. The results of our numerical simulations show that it is not possible to use the thus found attenuation directly for calculations of the line-length density. The line-length densities in these experiments can be calculated by using the ratios of the perpendicular and parallel vortex line-length densities in different systems. Since our results show also a difference in structure between a system with flat flow profile and Poiseuille flow it is necessary to determine first which flow type is the correct one for which experiment.

ACKNOWLEDGMENTS

This work was partly supported by the Dutch Foundation for the Fundamental Research on Matter (FOM), which is financially supported by the Dutch Organization for the Advancement of Research (NWO). This work was also sponsored by the "Stichting Nationale Computerfaciliteiten" (National Computing Facilities Foundation, NCF) for the use of supercomputer facilities, with financial support from the Dutch Organization for the advancement of Research (NWO).

¹ R.J. Donnelly, *Quantized Vortices in Helium II* (Cambridge University Press, Cambridge, 1991).

² R.T. Wang, C.E. Swanson, and R.J. Donnelly, *Phys. Rev. B* **36**, 5240 (1987).

³ K.W. Schwarz, *Phys. Rev. B* **38**, 2398 (1988).

⁴ R.G.K.M. Aarts and A.T.A.M. de Waele, *Phys. Rev. B* **50**, 10 069 (1994).

⁵ W.F. Vinen, *Proc. R. Soc. London, Ser. A* **240**, 114 (1957).

⁶ H.C. Kramers, T.M. Wirada, and A. Broese van Groenou, in *Proceedings of the VII International Conference on Low Temperature Physics, Toronto*, edited by G. M. Graham

and A.C. Hollis-Hallet (North-Holland, Amsterdam, 1960).

⁷ R.G.K.M. Aarts, Ph.D. thesis, Eindhoven University of Technology, 1993.

⁸ J.T. Tough, in *Progress in Low Temperature Physics*, edited by D. F. Brewer (North-Holland, Amsterdam, 1982), Vol. 8, p. 133.

⁹ K.W. Schwarz, *Phys. Rev. B* **18**, 245 (1978).

¹⁰ D.C. Samuels, *Phys. Rev. B* **46**, 11 714 (1992).

¹¹ A. Pierce, *Acoustics: An Introduction to its Physical Principles and Applications* (McGraw-Hill, New York, 1990).

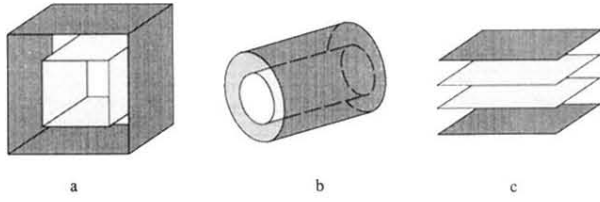


FIG. 1. The simulated geometries with their inner volumes, (a) the square tube (b) the circular tube, and (c) the slit.

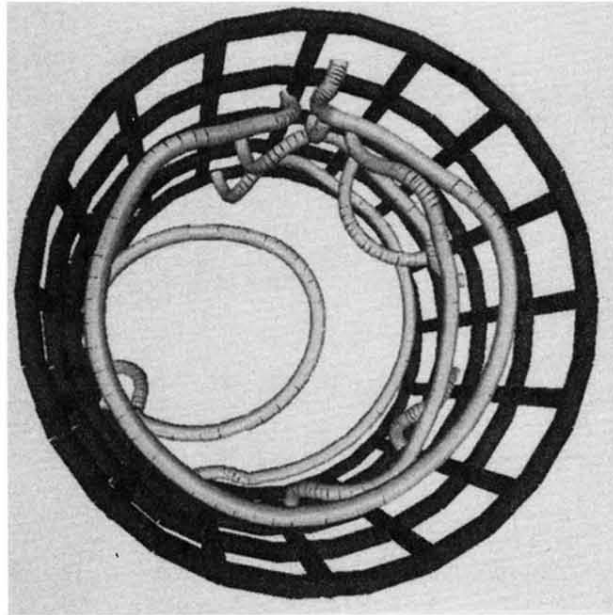


FIG. 2. Example of the vortex configuration in a circular tube with Poiseuille flow in equilibrium. The solid wall of the tube is here represented by a grid.